



Nano-pore structure characterization of shales using gas adsorption and mercury intrusion techniques

Liu Jun-yi, Qiu Zheng-song, Huang Wei-an, Luo Yang and Song Ding-ding

College of Petroleum Engineering in China University of Petroleum, Qingdao, China

ABSTRACT

In contrast to conventional reservoirs, gas shales have very low porosity and low permeability (in nano-darcy range), and shale matrix possesses ruleless pore structure and a wide pore size distribution with a significant pore volume in the nano-pore range. The nano-pore structure of gas shale plays an important role in hydrocarbon storage and transport. The low-pressure gas adsorption and high-pressure mercury intrusion techniques are adopted for nano-pore structure characterization of the Upper Triassic Xujiahe Formation in the Sichuan Basin. According to the results, the nano-pore geometry of shale samples is relatively complex, mainly slit-shaped. The pore size distribution suggests multi-modal with a broad peak between 2 nm and 30 nm, and the pore volume is predominantly occupied by meso-pores (2~50 nm) and the main specific surface area is dominated by the micro-pores (<2 nm) and meso-pores (<50 nm). Characterization of nano-pore structure is of great importance for the percolation mechanism and reservoir evaluation study of shale gas.

Keywords: Gas adsorption, mercury intrusion, shale, nano-pore structure, specific surface area.

INTRODUCTION

The matrix pore structure of shale gas and tight gas reservoirs, an important role in hydrocarbon storage and transport, is too difficult to characterize accurately because of a predominant portion of nano-pores associated with clays and organic matter [1]. Characterization of nano-pore structure is of great importance for the percolation mechanism and reservoir evaluation study of shale gas [2,3].

For conventional reservoirs, mercury intrusion technique is commonly used for pore structure analysis. But for unconventional gas reservoirs, much higher pressure could be required for mercury to be injected into the nano-pores [4], and high-pressure mercury intrusion technique is adopted mainly for analysis of macro-pores (>50 nm), avoiding distortion of pore structure under high pressure. Historically, low-pressure gas adsorption, nitrogen and carbon dioxide, has used for characterization of porous materials, and key parameters, such as surface area, pore volume and pore size distribution, could be acquired at the same time [5,6]. Low-pressure N₂ adsorption could be used for characterization of meso-pore (2~50 nm) and macro-pore, while low-pressure CO₂ adsorption could be used for characterization of micro-pore (<2 nm).

In this work, we have investigated the pore structure of Upper Triassic Xujiahe Shale in the Sichuan Basin using a combination of low-pressure N₂/CO₂ adsorption and high-pressure mercury intrusion, and the surface area, pore volume and pore size distribution were also calculated and compared based on difficult methods.

EXPERIMENTAL SECTION

Materials

The core shale samples in this paper were drilled from Upper Triassic Xujiahe Shale in the Sichuan Basin. The eight samples were numbered as SC-1~SC-8. Unlike previous published studies, core samples, not crushed samples, were used here for characterization of original pore structure.

Experimental methods

The N₂ adsorption isotherms and CO₂ adsorption isotherms were acquired at 77.3 K, 273.15 K respectively, by use of 3H-2000PS-RC Specific Surface Area and Pore Size Analyzer. The Brunauer Emmet Teller (BET) and Barrett Joyner Halenda (BJH) Theory were adopted for interpretation of N₂ adsorption data, while the Density Functional Theory (DFT) was adopted for interpretation of CO₂ adsorption data [7]. Mercury intrusion experiment was performed on AutoPore-IV-9505 Porosimeter. Its maximum allowable working pressure is 228 MPa and measuring range falls between 5 nm and 360 μm.

RESULTS

Low-pressure gas adsorption

Adsorption isotherms. Figure 1 depicts the N₂ adsorption and desorption isotherms of eight shale samples, and the each two branches all form a hysteresis loop with a specific shape. In general, according to the Brunauer, Deming, Deming and Teller classification [8], the N₂ adsorption isotherms belong to Type II, indicative of multilayer adsorption. At low relative pressure ($p/p_0=0\sim 0.2$), the gas adsorption volume increases significantly, and it forms the monolayer adsorption. At relative pressure below 0.8, the monolayer adsorption begins to shift to multilayer adsorption. As relative pressure increases above 0.8, the gas adsorption volume increases again, suggesting capillary condensation phenomenon. It is worthwhile to note that a significant portion of gas adsorption at relative pressure below 0.05 for all eight shale samples is indicative of micro-pores of nanometers range.

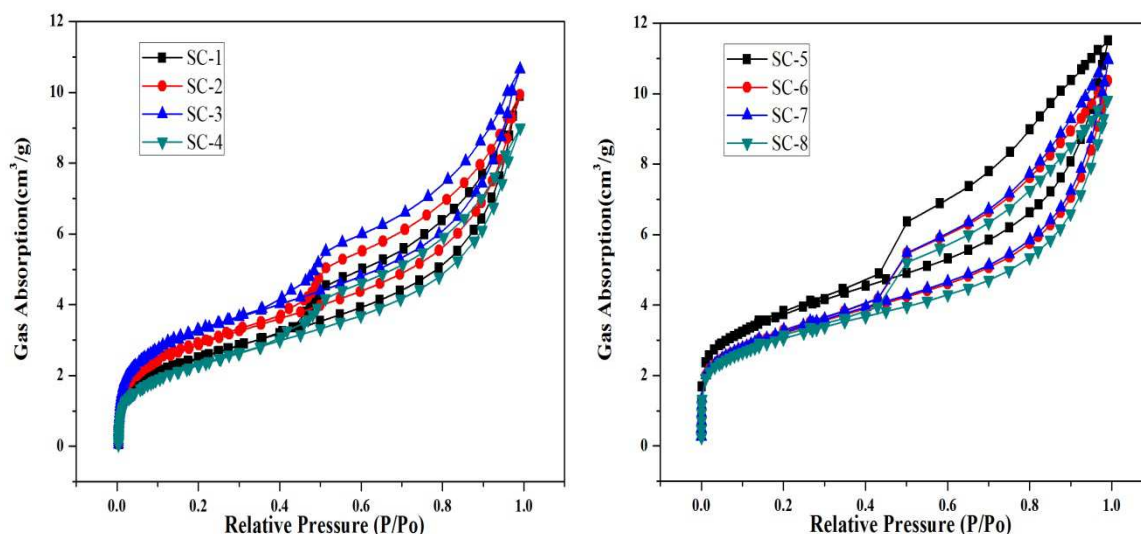


Fig. 1 N₂ adsorption isotherms of shale samples

The CO₂ adsorption isotherms of samples SC-1~SC-4 are shown in Figure 3. According to the Brunauer, Deming, Deming and Teller classification, the CO₂ adsorption isotherms belong to Type I, which is indicative of monolayer adsorption. The sample SC-3 displays the highest gas adsorption volume, suggesting the much more micro-pores.

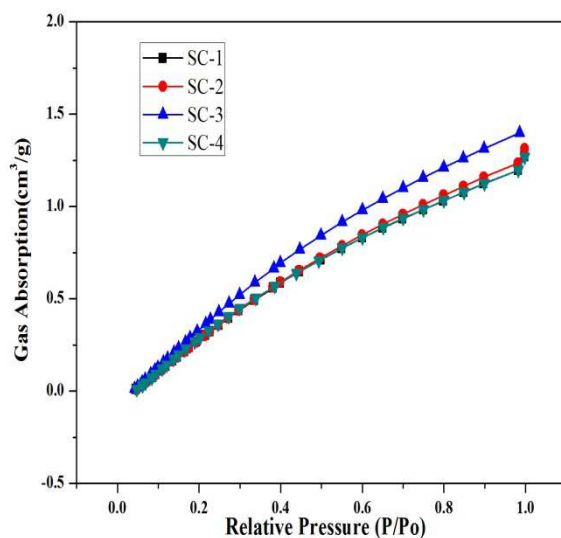


Fig. 2 CO₂ adsorption isotherms of shale samples

Surface area and pore volume. Based on the BET modal [9], the surface area and pore volume were obtained from N₂ adsorption data (Fig. 3). The sample SC-5 exhibits the highest surface area (12.91 m²/g) and pore volume (0.0179 cm³/g), and the average surface area and pore volume of eight samples are 10.72 m²/g, 0.0159 cm³/g respectively.

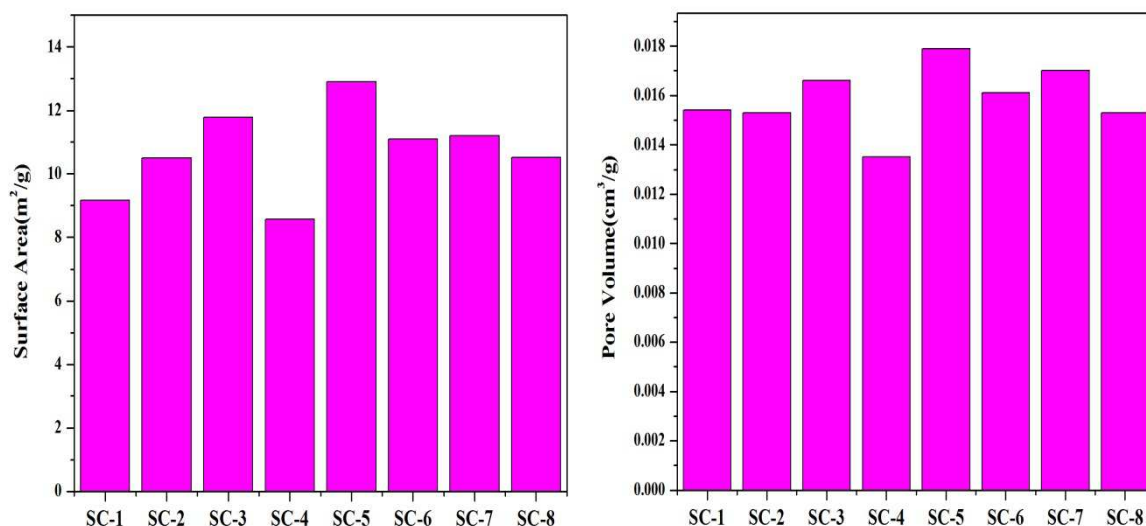


Fig. 3 Surface area and pore volume of shale samples

According to the IUPAC classification for pore sizes [10], the surface area and pore volume were compared in different range of pore size distribution, such micro-pore (<2 nm), meso-pore (2~50 nm) and macro-pore (>50 nm). As shown in Figure 4, for Xujiahe shale samples, a predominant portion (73.38%) of pore volume is occupied by meso-pores, and the portion occupied by micro-pores and macro-pores are only 14.75%, 10.18% respectively. The main specific surface area is dominated by the micro-pores (47.84%) and meso-pores (51.65%).

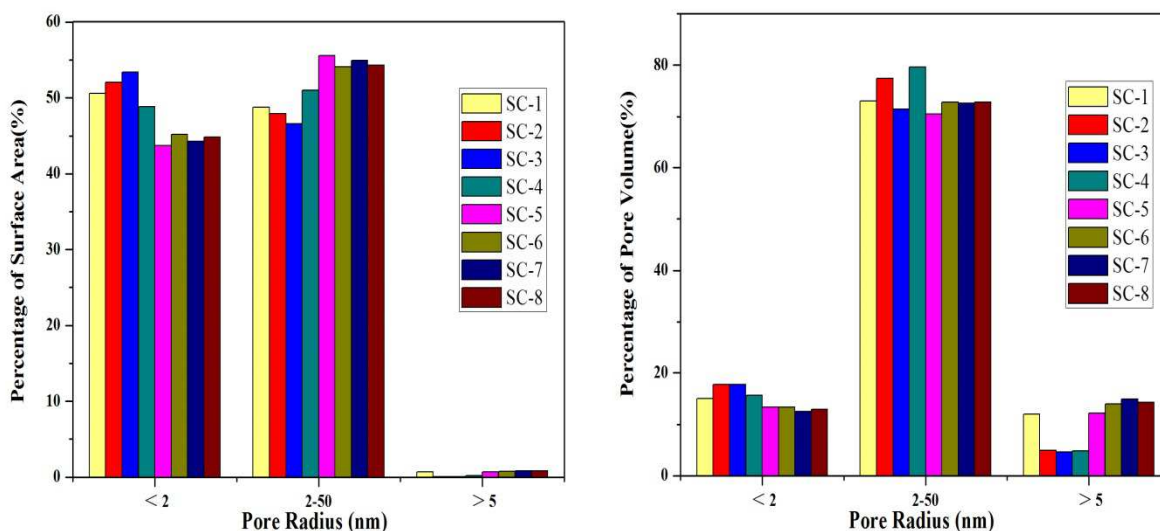


Fig. 4 Histogram analysis of specific surface area and pore volume

Pore size distribution. In contrast to conventional reservoirs, gas shales have very low porosity and low permeability (in nano-darcy range), and shale matrix possesses ruleless pore structure and a wide pore size distribution with a significant pore volume in the nano-pore range [11]. The pore size distribution plots (Fig. 5) were obtained from N_2 adsorption data according to Barrett Joyner Halenda (BJH) Theory. It could be seen obviously from figure 5 that the plots show a multi-modal distribution with modes at around 1.5~2.5 nm, 15~18 nm and 26~34 nm. The average pore size of samples mainly falls into the range of 5.55~6.73 nm with an average pore size of 5.97 nm.

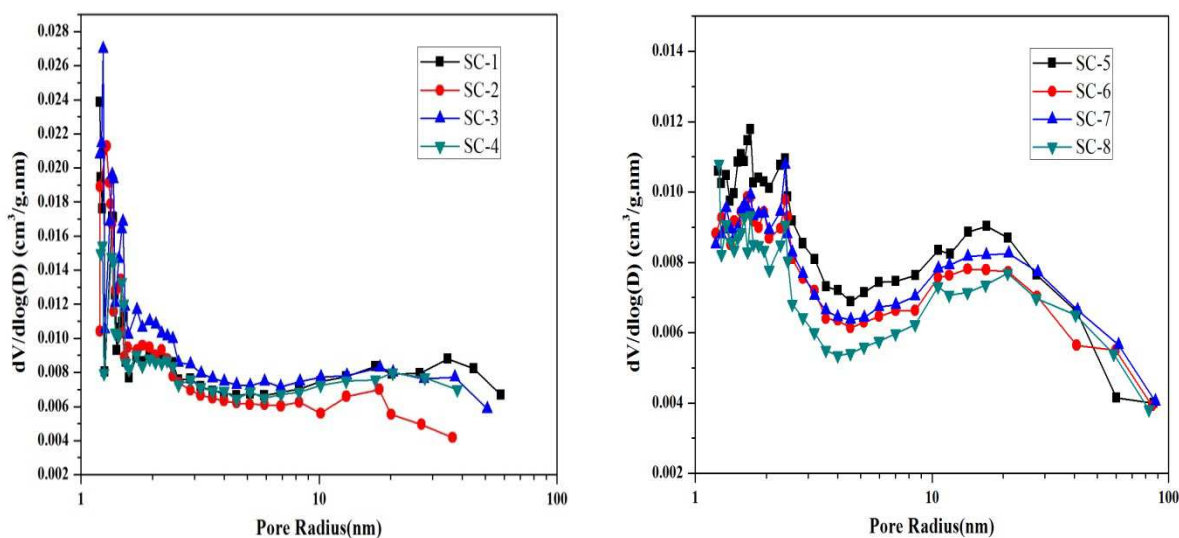


Fig. 5 Pore size distribution plots from adsorption data of shale samples

It is worth noting that the pore size distribution plots from N_2 desorption data appear to display a false peak at around 3.6 nm (Fig. 6) due to the tensile strength effect [12]. Therefore, it is reasonable to obtain the pore size distribution from gas adsorption data.

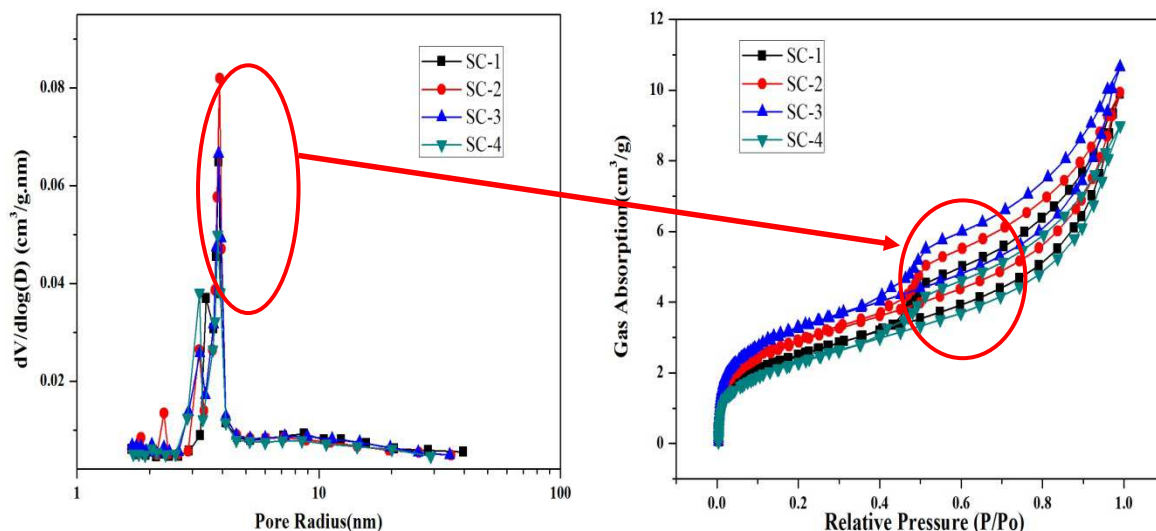
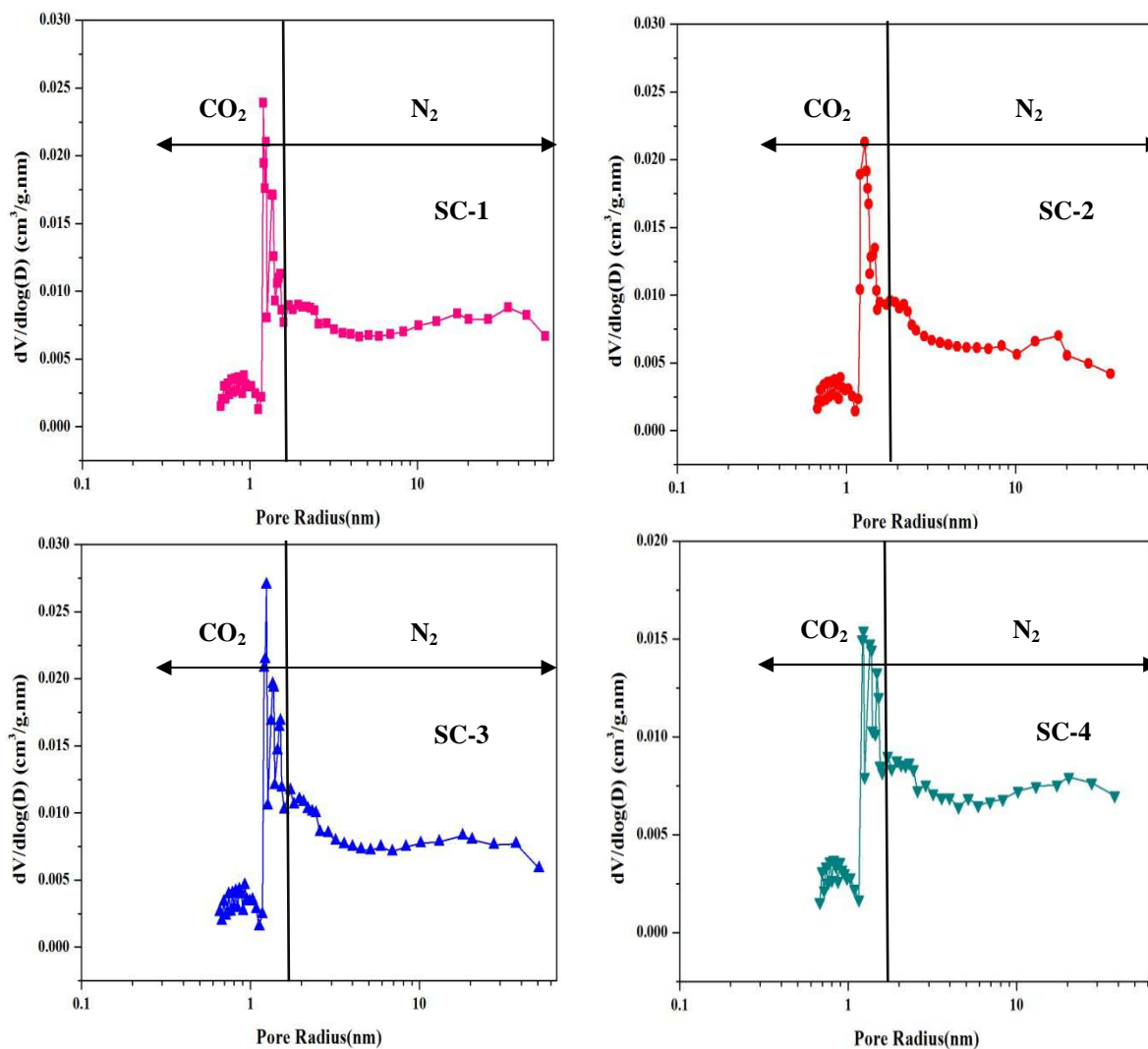


Fig. 6 Pore size distribution plots from desorption data of shale samples

Fig. 7 Pore size distribution plots from N_2 and CO_2 adsorption data

As discussed by Clarkson et al [13], micro-pore could be characterized by CO_2 adsorption at 273.15 K, while meso-pore and macro-pore could be characterized by N_2 adsorption at 77.3 K. In other words, combination of CO_2 and N_2 adsorption data could be used to obtain a wide pore size distribution of shale samples. Taking samples SC-1~SC-4

as examples, the continuity of the CO₂ and N₂ pore size distribution plots is exhibited clearly in figure 7, and the CO₂ and N₂ pore size distribution plots display a smooth transition at 1 nm, thus providing the more comprehensive pore size distribution of shale samples.

High-pressure mercury intrusion

The cumulative and incremental pore size distribution plots (Fig. 8) from high-pressure mercury intrusion data exhibit a wide pore size distribution, mainly in the meso-pore and macro-pore range. The incremental plots show multi-modal distribution for samples SC-5~SC-8, with modes at around <3 nm and 12~30 nm. All four samples display an additional peak at around 3~10 nm, which is related to the micro-fractures or stress-relaxation fractures (Fig. 9).

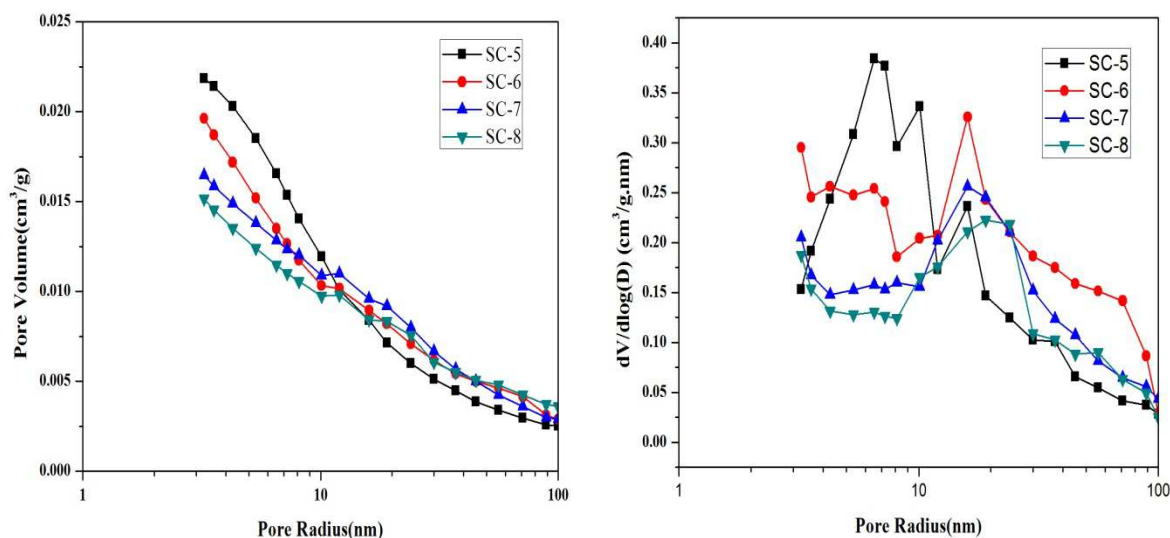


Fig. 8 Cumulative and incremental pore size plots from mercury intrusion data

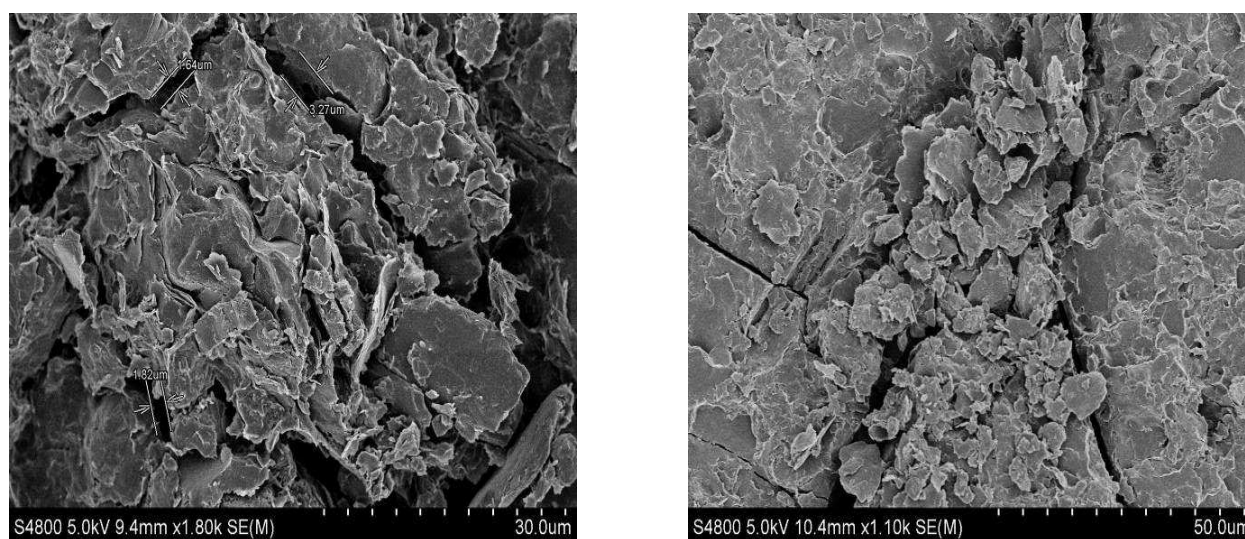


Fig. 9 The SEM photos of shale samples

DISCUSSION

Due to capillary condensation phenomenon, the gas adsorption and desorption branches would not coincide each other, forming a hysteresis loop with a specific shape. The characters of a hysteresis loop are dependent on the pore structure. The International Union of Pure and Applied Chemistry (IUPAC) proposed four classification standard loops (H1, H2, H3, H4) and its corresponding pore type (Fig. 10) [14]. Obviously, it is difficult to characterize the actual pore structure using one classification standard loop because of the complex structure of rock and other porous materials. Therefore, when the actual hysteresis loop is similar to one of the four classification standard loops, the pore structure could be confirmed approximately [15].

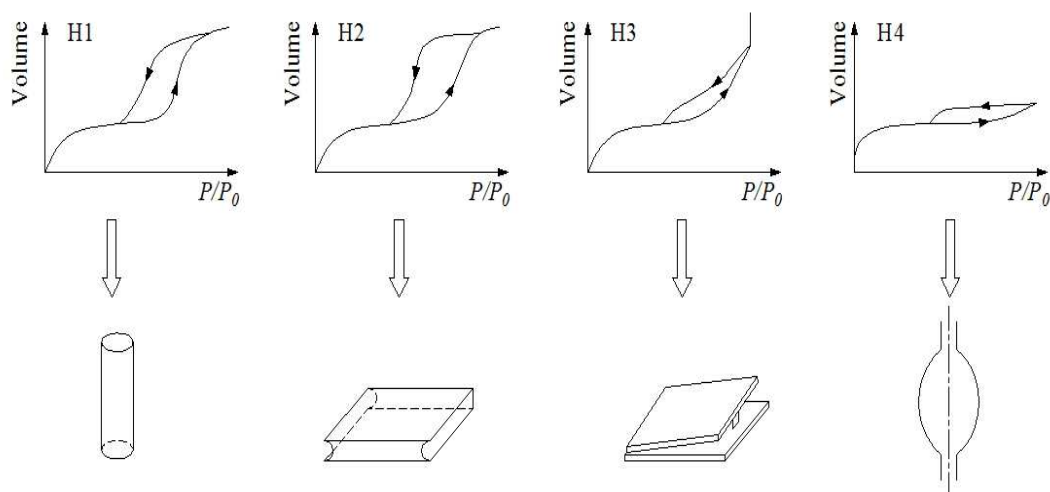


Fig. 10 Classification of hysteresis loops and pore types recommended by IUPAC

Generally, the hysteresis loops of Xujiahe Shale samples are similar to the H3 classification standard loop, but not the exactly same. The actual hysteresis loop usually suggests the synergistic effect of a variety of pore geometries. Based on the analysis above, the pore geometry of Xujiahe Shale samples is interpreted to be slit-shaped on the whole, and other pore geometries also exist. What's more, the pores of Xujiahe Shale samples are mainly accessible because the semi-closed or closed pores would not form hysteresis loops.

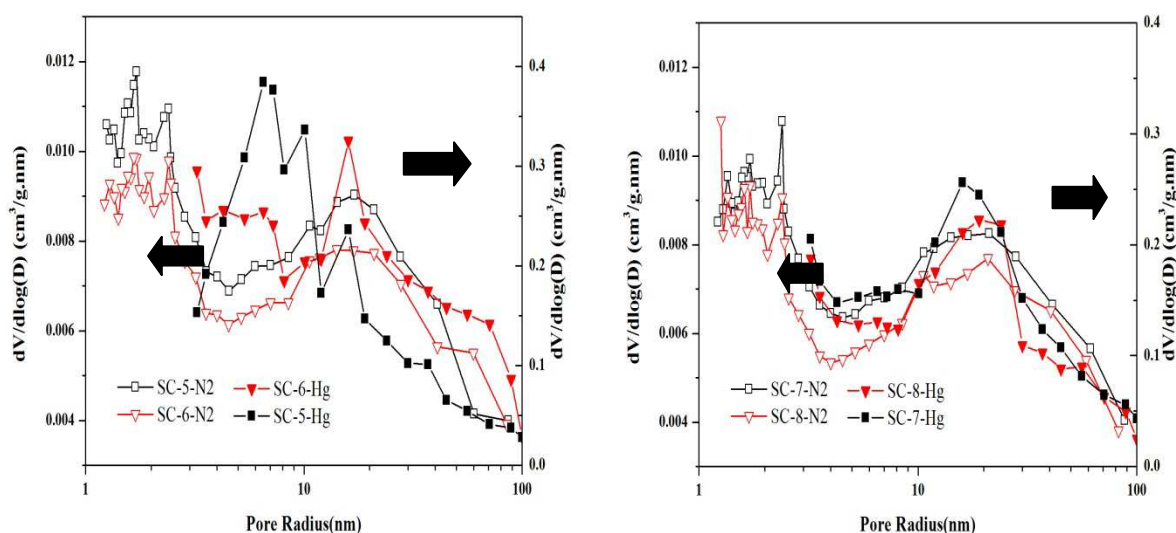


Fig. 11 Comparison of pore size distribution plots from N₂ adsorption and mercury intrusion data

As shown in figure 11, the pore size distribution from N₂ adsorption and mercury intrusion data were compared and the agreement between them was reasonable, especially for sample SC-7, SC-8. Although the two curves were not the exactly same because mercury intrusion measures the pore throats and gas adsorption measures the pore bodies, the agreement between N₂ adsorption and mercury intrusion data further suggests the pore geometry of Xujiahe Shale samples are slit-shaped, in this case that the gas adsorption and mercury intrusion have similar results because the pore throats are the same as pore bodies.

CONCLUSION

Low-pressure N₂/CO₂ adsorption and high-pressure mercury intrusion techniques were combined to characterize the pore structure of Xujiahe Shale samples, providing the more comprehensive pore size distribution of shale samples. According to the results, the nano-pore geometry of shale samples is relatively complex, mainly slit-shaped. The pore size distribution suggested multi-modal with a broad peak between 2 nm and 30 nm, and the pore volume is predominantly occupied by meso-pores and the main specific surface area is dominated by the micro-pores and meso-pores.

Acknowledgements

We would like to thank the financial support from National Science and Technology Major Project of China (2011ZX05005-006-007HZ) and the Graduate Innovation Project of China University of Petroleum (East China) (YCX2014006).

REFERENCES

- [1] Bustin R M, Bustin A M M, Cui X, et al. Impact of shale properties on pore structure and storage characteristics. *SPE* 119892, **2008**.
- [2] ZOU Cai-neng, ZHU Ru-kai, BAI Bin, et al. *Acta Petrologica Sinica*, **2011**, 27(6): 1857-1864.
- [3] Clarkson C R, Jensen J L, Blasingame T A. Reservoir engineering for unconventional gas reservoirs: what do we have to consider. *SPE* 145080, **2011**.
- [4] TIAN Hua, ZHANG Shui-chang, LIU Shang-bo, et al. *Acta Petrolei Sinica*, **2012**, 33(3): 419-427.
- [5] YANG Kan, LU Xian-cai, LIU Xian-dong, et al. *Bulletin of Mineralogy, Petrology and Geochemistry*, **2006**, 25(4): 362-368.
- [6] Ambrose R J, Hartman R C, Diaz-Campos Mery, et al. New pore-scale consideration for shale gas in place calculations. *SPE* 131772, **2010**.
- [7] Clarkson C R, Solano N, Bustin R M, et al. *Fuel*, **2012**, 103: 606-616.
- [8] Brunauer S, Deming L S, Deming W S, et al. *J Am Chem Soc*, **1940**, 62: 1723-1732.
- [9] ISO 9277:2010, Determination of the specific surface area of solids by gas adsorption-BET method.
- [10] Rouquerol J, Fairbridge C W, Everett D H, et al. *Pure and Analytical Chemistry*, **1994**, 66(8): 1739-1758.
- [11] Bowker K A. *Geological Society Bulletin*, **2003**, 42(6): 1-11.
- [12] CHEN Yong. Preparation and characterization of porous materials. Beijing: Press of University of Science and Technology of China, **2010**: 69-76.
- [13] Clarkson C R, Wood J M, Aquino S D, et al. Nanopore structure analysis and permeability predictions for a tight gas/shale reservoir using low-pressure adsorption and mercury intrusion techniques. *SPE* 155537, **2012**.
- [14] Rouquerol F, Rouquerol J, Sing K. Adsorption by powers and porous solids: principles, methodology and application. London: Academic Press, **1999**.
- [15] CHEN Shang-bin, ZHU Yan-ming, WANG Hong-yan, et al. *Journal of China Coal Society*, **2012**, 37(3): 439-445.